

Optically Transparent Au{111} Substrates: Flat Gold Nanoparticle Platforms for High-Resolution Scanning Tunneling Microscopy

Daminda H. Dahanayaka, Jane X. Wang, Sohrab Hossain, and Lloyd A. Bumm*

Center for Semiconductor Physics in Nanostructures, Homer L. Dodge Department of Physics and Astronomy, The University of Oklahoma, 440 West Brooks Street, Norman, Oklahoma 73019

Received February 5, 2006; E-mail: bumm@nhn.ou.edu

In the last two decades, Au{111} substrates have become widely used for surface modification,¹ nanolithography,^{2,3} and single molecule studies^{4,5} because of the broad applicability of alkanethiol self-assembled monolayer (SAM) chemistry. Typically, these substrates are Au{111} oriented thin films on mica⁶ or Au{111} surfaces of bulk single crystals, which are both commercially available. Because these substrates are opaque, optical access is restricted to the front side, which complicates simultaneous electrical and optical investigation on Au{111} substrates. We recently developed a new type of Au{111} substrate which is transparent (allows optical access from front and back)⁷ and is suitable for high-resolution STM. This substrate consists of solution-grown flat gold nanoparticles (FGNPs) that are deposited on indium tin oxide (ITO)-coated glass. The transparent ITO support allows optical access to the FGNP substrates, which exhibit plasmon resonance modes extending well into the NIR region. These FGNP/ITO substrates have the benefits of low cost, simple preparation, and broad applicability. We also anticipate that the plasmon resonances of the FGNPs will facilitate optical coupling to the adsorbed molecules. We propose that these substrates can be generally applied as atomically flat Au{111} substrates for scanning probe microscopy and that the FGNPs will find application as nanometer-scale platforms.

High-resolution STM imaging imposes several stringent criteria on the substrates. The substrate must be atomically flat, or be composed of atomically flat terraces large enough for imaging. This is necessary, otherwise the surface roughness will swamp out the molecular corrugation of the SAM and also can lead to disorder of the SAM. This practically limits our choice to single crystals. The substrate must also be in electrical contact to the STM electronics and, for our purposes, also optically transparent. ITO-coated glass is a readily available supporting substrate for the FGNPs, which is both optically transparent and electrically conducting. Although the ITO coating is rough at the nanometer scale, the FGNPs ride on the ITO and provide the required atomically flat surfaces.

The FGNPs are prepared by adding 1.2 mL of 48 mM citric acid solution to 95 mL of 0.24 mM HAuCl₄ solution at 4 °C (refrigerator). The particles grow over a period of 3–4 days. The resulting sol is polydisperse, consisting of large flat triangles, hexagons, and intermediate shapes along with spheroidal particles. The flat particles are single crystals which range in lateral size from tens to thousands of nanometers but are only 15–20 nm thick. Our procedure is a variant of the standard citrate sol described by Turkevich,⁸ reducing HAuCl₄ with citric acid.⁹

The FGNPs are deposited on ITO-coated glass substrates by centrifugation. Freshly cleaned ITO substrates were placed ITO side up at the bottom of a test tube filled with the Au sol containing the FGNPs, and centrifuged in a swinging-bucket rotor for 10 min at 600–1500g (min/max *g* values at the inner/outer radius). Centrifugation deposits all the particles onto the ITO surface. The resulting

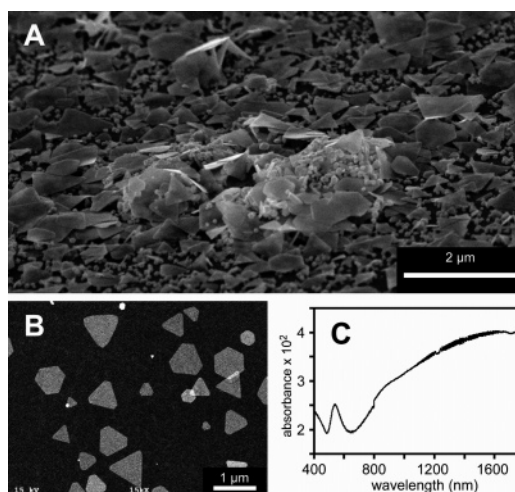


Figure 1. (A) SEM image before ultrasonication of the crude FGNPs on ITO. (B) SEM image of the measurement-ready substrate after 5 min of ultrasonication; the surface has been cleaned of spheres, aggregates, and poorly contacted FGNPs. (C) Vis–NIR extinction spectrum of the FGNP/glass substrate prepared as in B. The glitch at 800 nm is an artifact due to a grating change. The fine structure above 1000 nm is due to optical interference from multiple reflections within the glass substrate. The peak at 540 nm is due to residual spheroidal particles.

reddish brown layer of nanoparticles is visible by eye. Figure 1A is an SEM image of this very dense layer containing FGNPs, Au spheroids, and aggregates. Ultrasonication in deionized water for a few minutes removes the spheres and aggregates leaving the FGNPs (Figure 1B). Longer ultrasonication times do not dramatically affect the results. The ultrasonication step is so efficient that our initial efforts to separate the FGNPs from the spheroids proved unnecessary. We hypothesize that the FGNPs are more strongly bound than the spheres due to their larger contact area. These substrates constitute our measurement-ready samples.

Extinction spectra of FGNPs on glass show that the plasmon resonances of the FGNPs extend well into the NIR. The polydispersity of the FGNPs produces the broad extinction band beginning above 600 nm and extending out past 1600 nm. This region includes the dipole, quadrupole, and higher modes.^{10,11}

STM images of the FGNPs typically show that only 3–4 atomic layers are exposed at the surface (Figure 2A). The topmost exposed layers are islands, and the lowest exposed layers are vacancy islands. In all cases we have observed, the island step edges are meandering steps. We only observe low index step edges at the edges of the FGNP. Furthermore, the islands are distributed uniformly across the FGNP surface, indicating that the thickness is uniform across the particle. Note that the ITO surface is very rough at the nanometer scale, which is typical for sputtered polycrystalline films. Despite the roughness of the ITO supporting substrate, the FGNPs remain flat for high-quality STM imaging.

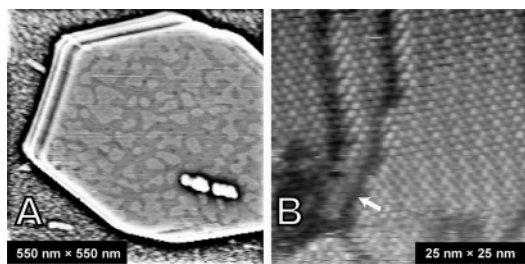


Figure 2. (A) STM image of a hexagonal FGNP showing the atomic terraces. The image has been high-pass spatial filtered to bring out the detail on the FGNP and ITO surfaces. The defect on the FGNP surface was caused by a tip crash. The steps visible at the edge of the FGNP are tip artifacts caused by the abrupt edge of the particle. These artifacts are common in scanned probe microscopy when the probe tip scans a large amplitude feature (the edge in this case) that is much sharper than the probe tip. STM images of the top surface of the FGNP are not affected. (B) A high-resolution zoom on the surface of the FGNP shown in A. The corrugation is the $\sqrt{3} \times \sqrt{3} R30^\circ$ molecular lattice characteristic of well-ordered alkanethiol SAMs. The dark features (arrow) are SAM structural domain boundaries. (The tunneling condition for both images are: $-1 V_{\text{sample}}$, 1 pA .)

SAMs were prepared by immersing the ITO-supported FGNPs in a 1 mM ethanolic solution of 1-decanethiol for 24 h or grown by vapor phase exposure to the thiol vapor at 60°C . Initially, we were concerned that the FGNPs would release from the surface during SAM growth. However, we have found the substrates to be quite robust to solution processing. SAMs grown on the FGNPs show the characteristic $\sqrt{3} \times \sqrt{3} R30^\circ$ and related superstructures of alkanethiolates on Au{111} (Figure 2B).^{1,5}

AFM measurements of other groups^{10,12} have shown that FGNPs are atomically flat; however, they did not resolve the atomic terraces. To our knowledge, this is the first report of high-resolution STM imaging of the atomic terraces on nanoparticles or molecularly resolved imaging of SAMs on a nanoparticle. It is noteworthy that we have been unable to obtain high-resolution STM images of FGNPs grown with poly(vinylpyrrolidone) (PVP) or grown as described herein and subsequently stabilized with PVP. We suspect that PVP is not easily displaced by the alkanethiolate SAM, in contrast to a small molecule, such as citrate. It is no surprise that we do not observe adsorbed PVP molecules by STM because they are expected to be highly disordered and fluxional. By contrast, alkanethiolate molecules in a well-ordered SAM are sterically locked.

Unlike the typical Au{111} substrates, these substrates are not completely covered by Au. Thus, FGNP density is a criterion not to be overlooked for supported nanoparticle surfaces. Specifically, at least one FGNP should lie within the scan range of the STM. For our system with a $10 \mu\text{m} \times 10 \mu\text{m}$ scan range, we find that a density of approximately 10 particles per $100 \mu\text{m}^2$ is adequate to quickly find a particle. The density of FGNPs can be reduced by diluting the sol before centrifugation or increased by multiple centrifugation–ultrasonication cycles. Although the density is not uniform because the particles arrange randomly, we typically have no trouble locating FGNPs with this procedure. Occasionally, it will be necessary to explore a few $10 \mu\text{m} \times 10 \mu\text{m}$ scan ranges before finding an FGNP, but this inconvenience is more than offset by the simplicity of preparation.

We have found that a very effective imaging strategy is to first locate an FGNP using large ($1\text{--}2 \mu\text{m}$) low-resolution scans. The

distance between the scan lines should be less than half the size of the smallest particle desired. Once an FGNP is located, the tip is moved directly onto the FGNP and the experiments using the FGNP as a single-crystal atomically flat Au{111} substrate can begin. Ironically, the more difficult experiment is to acquire good large area images, such as shown in Figure 2A. This is because our STM scan head is optimized for atomic-scale imaging.

In summary, we have successfully demonstrated FGNP/ITO substrates as a viable substrate for high-resolution STM measurements. These substrates are low cost compared to Au single crystals and commercial Au{111}/mica substrates.¹³ The preparation of the FGNP/ITO substrates employs basic wet chemical techniques and does not require costly specialized equipment as do Au{111}/mica substrates. These substrates can be applied broadly as inexpensive, “easy-to-prepare” Au{111} substrates for STM. One distinct advantage of these substrates is their ability to support electrical and optical measurements simultaneously with excellent optical access. Although our emphasis has been to develop substrates that satisfy the very stringent requirements of high-resolution STM (electrically conductive, single crystalline, and atomically flat), these substrates can also be used for other SPM techniques (AFM, NSOM, etc.). If electrical conductivity and/or optical transparency is not required, other substrates can be substituted. For non-STM applications, we have had success using a variety of substrates, including borosilicate microscope slides, mica, sapphire, and silicon with native oxide. These substrates should prove to be valuable for a wide variety of SPM and optical experiments.

Acknowledgment. D.H.D. thanks Oklahoma EPSCoR and CSPIN for a graduate research fellowship. We thank William Chisoe, III and Preston R. Larson for electron microscopy. We thank Barry K. Lavine, David J. Westover, and Necati Kaval for use of the Cary 6000. This work was supported by the National Science Foundation CAREER Grant No. CHE-0239803, the Center for Physics in Nanostructures, NSF MRSEC No. DMR-0080054, and Oklahoma EPSCoR.

References

- (1) Love, J. C.; Estroff, L. A.; Kriebel, J. K.; Nuzzo, R. G.; Whitesides, G. M. *Chem. Rev.* **2005**, *105*, 1103–1169.
- (2) Liu, G.; Xu, S.; Qian, Y. *Acc. Chem. Res.* **2000**, *33*, 457–466.
- (3) Ginger, D. S.; Zhang, H.; Mirkin, C. A. *Angew. Chem., Int. Ed.* **2004**, *43*, 30–45.
- (4) Dunbar, T. D.; Cygan, M. T.; Bumm, L. A.; McCarty, G. S.; Burgin, T. P.; Reinert, W. A.; Jones, L.; Jackiw, J. J.; Tour, J. M.; Weiss, P. S.; Allara, D. L. *J. Phys. Chem. B* **2000**, *104*, 4880–4893.
- (5) Poirier, G. E. *Chem. Rev.* **1997**, *97*, 1117–1127.
- (6) Chidsey, C. E. D.; Loiacono, D. N.; Sleator, T.; Nakahara, S. *Surf. Sci.* **1988**, *200*, 45–66.
- (7) Window-like transparency of the FGNPs is not required because the particle size is on the order of the wavelength of light. Light incident on, or emanating from, one side of the FGNP does not remain localized on that side, but will excite plasmon modes of the entire particle.¹¹
- (8) Turkevich, J.; Stevenson, P. C.; Hillier, J. A. *Discuss. Faraday Soc.* **1951**, *11*, 55–75.
- (9) Chiang, Y.; Turkevich, J. *J. Colloid Sci.* **1963**, *18*, 772–783.
- (10) Millstone, J. E.; Park, S.; Shuford, K. L.; Qin, L.; Schatz, G. C.; Mirkin, C. A. *J. Am. Chem. Soc.* **2005**, *127*, 5312–5313.
- (11) Shuford, K. L.; Ratner, M. A.; Schatz, G. C. *J. Chem. Phys.* **2005**, *123*, 114713.
- (12) Shankar, S. S.; Rai, A.; Ankamwar, B.; Singh, A.; Ahmad, A.; Sastry, M. *Nat. Mater.* **2004**, *3*, 482–488.
- (13) Molecular Imaging, 4666 S. Ash Avenue, Tempe, AZ 85282 (<http://www.molec.com/>).

JA060862L